Published in final edited form as:
Immunity. 2011 September 23; 35(3): 388–399. doi:10.1016/j.immuni.2011.07.007.

The Signaling Adaptor Eps8 Is an Essential Actin Capping Protein for Dendritic Cell Migration

Emanuela Frittoli[1,5], **Gianluca Matteoli**[2,5,7], **Andrea Palamidessi**[1,6], **Elisa Mazzini**[2,6], **Luigi Maddaluno**[1], **Andrea Disanza**[1], **Changsong Yang**[4], **Tatyana Svitkina**[4], **Maria Rescigno**[2,*], and **Giorgio Scita**[1,3,*]

[1]IFOM, FIRC Institute of Molecular Oncology Foundation at IFOM-IEO Campus, Via Adamello 16, 20139 Milan, Italy

[2]IEO, Department of Experimental Oncology, European Institute of Oncology, Via Ripamonti 435, 20141 Milan, Italy

[3]Dipartimento di Medicina, Chirurgia ed Odontoiatria, Università degli Studi di Milano, 20142 Milan, Italy

[4]Department of Biology, University of Pennsylvania, Philadelphia, PA 19104, USA

Abstract

Dendritic cells (DCs) flexibly adapt to different microenvironments by using diverse migration strategies that are ultimately dependent on the dynamics and structural organization of the actin cytoskeleton. Here, we have shown that DCs require the actin capping activity of the signaling adaptor Eps8 to polarize and to form elongated migratory protrusions. DCs from Eps8-deficient mice are impaired in directional and chemotactic migration in 3D in vitro and are delayed in reaching the draining lymph node (DLN) in vivo after inflammatory challenge. Hence, Eps8-deficient mice are unable to mount a contact hypersensitivity response. We have also shown that the DC migratory defect is cell autonomous and that Eps8 is required for the proper architectural organization of the actin meshwork and dynamics of cell protrusions. Yet, Eps8 is not necessary for antigen uptake, processing, and presentation. Thus, we have identified Eps8 as a unique actin capping protein specifically required for DC migration.

INTRODUCTION

Dendritic cells (DCs) are essential for the initiation of the acquired immune response, during which they capture and present antigens, undergo maturation, and migrate from peripheral tissues to nearby lymph nodes to activate T cells (Randolph et al., 2008). To perform these functions, DCs flexibly adapt their adhesive, actin-based structures and migratory properties. For example, the migration of immature DCs from the bone marrow (BM), where they are produced, to peripheral tissues is thought to involve the formation of prototypical adhesive, actin-rich, and highly invasive podosomes (Pierre et al., 1997; West et al., 2004). Exposure to endogenous or exogenous “danger” signals induces the differentiation of DCs into a

*Correspondence: maria.rescigno@ifom-ieo-campus.it (M.R.), giorgio.scita@ifom-ieo-campus.it (G.S.).
[5]These authors contributed equally to this work
[6]These authors contributed equally to this work
[7]Present address: Department of Gastroenterology, University of Leuven, Herestraat 49 3000 Leuven, Belgium

SUPPLEMENTAL INFORMATION

Supplemental Information includes seven figures, Supplemental Experimental Procedures, and seven movies and can be found with this article online at doi:10.1016/j.immuni.2011.07.007.

motile state, which is associated with loss of adhesive structures and properties, including podosomes and integrin-based cell-matrix interactions (Pierre et al., 1997; West et al., 2004). These events enable DCs to adopt a flexible nonadhesive mode of motility driven mainly by protrusive actin flows at the cell front, while actomyosin contraction at the rear serves to squeeze and propel the nucleus through gaps in the extracellular matrix (ECM) (Lämmermann et al., 2008). Within this context, regulators of actin dynamics, including actin bundlers and capping proteins, are expected to play a critical role by controlling the architecture and dynamics of the actin meshwork that propels nonadhesive DC migration.

Among these molecules, Eps8 is a unique actin binding and signaling protein that possesses actin filament bundling and capping activities, the coordination of which is important for the generation of various types of protrusions in both sessile and highly migratory cells (Hertzog et al., 2010). Eps8 is the prototype of the Eps8L family of capping proteins, which includes four related and functionally redundant genes in mammals (Disanza et al., 2004; Offenhäuser et al., 2004). Eps8L molecules display a modular domain organization more typically found in signaling adaptors and scaffolds (Offenhäuser et al., 2004; Tocchetti et al., 2003). Accordingly, Eps8 participates in the formation of distinct macromolecular complexes that either transduce signals from Ras to Rac leading to actin remodeling or regulate endocytosis of receptor tyrosine kinases (Lanzetti et al., 2000; Scita et al., 1999). The isolated C-terminal domain (aa 648–821) caps barbed ends in the nanomolar range, but it is inhibited in the context of the full-length protein (Croce et al., 2004; Disanza et al., 2004). Unlike other cappers, full-length Eps8 has also been shown to organize actin filaments into higher-order structures, and this crosslinking activity is enhanced by interaction with insulin receptor tyrosine kinase substrate p53 (IRSp53) (Abbott et al., 1999; Disanza et al., 2006; Funato et al., 2004; Oda et al., 1999). The molecular basis of the capping and bundling activities of Eps8 have recently been unveiled; Eps8 can wrap around filaments, contacting the barbed end actin unit through an amphipathic helix that is essential for blocking the addition of further monomers, while extending its C-terminal globular core along the filament side in a configuration that allows Eps8 to crosslink filaments (Hertzog et al., 2010). Single-point mutagenesis has allowed the dissection of these distinct Eps8 activities both in vitro and in vivo, providing clues as to their functional relevance in cell migration and morphogenesis of actin structures, such as microvilli and stereocilia (Croce et al., 2004; Hertzog et al., 2010; Manor et al., 2011; Tocchetti et al., 2010).

On the basis of these considerations, we hypothesized that Eps8 may be critical in DC migration. Here, we show that Eps8 is expressed in DCs. Using an Eps8-deficient mouse model and in vitro assays of DC migration, we have demonstrated that Eps8 is essential for DC trafficking in vivo and DC migration in 2D and 3D in vitro. Eps8 mediates these processes by promoting, through its capping activity, the formation of a dense actin meshwork, which is, in turn, essential for sustaining persistent and extended cell protrusions. Thus, Eps8 is a critical capping protein for DC migration.

EXPERIMENTAL PROCEDURES

All animal experiments were conducted in accordance with national guidelines and were approved by the ethics committee of the Animal Welfare Office of the Italian Work Ministry and conformed to the legal mandates and Italian guidelines for the care and maintenance of laboratory animals.

In Vivo T Cell Proliferation Assay

Flow cytometry-purified $CD4^+CD25^-CD462L^+$ naive T cells isolated from spleen of OT-II TCR $Ly5.2^+$ mice were labeled with 1.25 μM CFSE. CFSE naive OT-II T cells (2 million) were injected intravenously in C57BL/6 $Ly5.1^+$ recipient mice. After 24 hr, 3×10^5 OVA-

loaded matured *Eps8*$^{-/-}$ or WT BMDCs were injected in the right or in the left footpad, respectively. After 3 days, popliteal DLNs were removed and T cells proliferation (CFSE dilution) was assessed by flow cytometry.

In Vitro Antigen Presentation to T Cell by BMDCs

$CD4^+CD25^-CD462L^+$ naive T cells isolated from spleen of OT-II TCR $Ly5.2^+$ mice were labeled with 5μM of CFSE and cocultured with *Eps8*$^{-/-}$ or WT OVA-loaded BMDCs for 3 or 5 days in round- or flat-bottom 96-well plates. T cells proliferation was assessed byCFSE dilution by flow cytometry. Supernatants were collected and cytokine content was analyzed with cytometric bead array in accordance with the manufacturer's instructions (BD Biosciences).

Contact Hypersensitivity

Contact hypersensitivity (CHS) was carried as described (Wang et al., 1997a). In brief, for sensitization, *Eps8*$^{-/-}$ or WT mice were painted (day 0) on shaved abdominal skin with 100 μl of 3% OXA in 4:1 acetone:olive oil solution. After 5 days, mice were challenged by the application of 10 μl of OXA (1%) on each side of the right ear, whereas the left ear received the vehicle alone. CHS response was determined by measuring the size of the antigen-painted ear compared to that of the vehicle-treated controlateral ear. The results are expressed as fold of size increase calculated over vehicle-treated controlateral ear. For histological analysis, mouse ears sections were stained with hematoxylin-eosin.

Trafficking to the DLNs of BMDC Injected into the Footpad

BMDCs from WT or *Eps8*$^{-/-}$ mice treated with 200 ng/ml LPS for 6 hr were labeled respectively with 5μM eFluor 670 or 5μM CFSE. WT and *Eps8*$^{-/-}$ BMDCs (1.5×10^5) at a 1:1 ratio were suspended in 20μL PBS and injected subcutaneously into the hind footpads of C57BL/6 mice. After 24 hr, popliteal DLNs were either digested so that cells suspensions could be obtained for flow cytometry analysis or frozen in cryomatrix and sectioned in 10 μm slices for immunofluorescence analysis.

Statistical Analysis

Student's paired t test was used for determining the statistical significance. Significance was defined as $*p < 0.05$; $**p < 0.01$; and $***p < 0.001$. Statistic calculations were performed with JMP 5.1 software (SAS Cary).

RESULTS

Eps8 Is Required for DC Elongated Cell Shape In Vitro and Migration to Lymph Nodes In Vivo

In mammals, Eps8 is a member of an Eps8L protein family that includes three additional highly conserved, functionally redundant gene products (Offenhäuser et al., 2004; Tocchetti et al., 2003). We, therefore, first examined the expression pattern of Eps8L mRNAs in bone marrow-derived DCs (BMDCs) of wild-type (WT) or Eps8-deficient mice. We detected significant amounts only of Eps8 mRNA, but not Eps8L1, Eps8L2 or Eps8L3 mRNAs in WT BMDCs (Figure S1A available online). Furthermore, genetic removal of *Eps*8 was not accompanied by a compensatory elevation of the mRNA of the other family members. Notably, Eps8 expression in spleen-derived DCs was far superior than that in other innate and adaptive immune cells, such as macrophages, neutrophils, and T and B cells (Figure S1B). Thus, Eps8 might play a unique nonredundant function in actin-based processes in BMDCs. Consistent with this latter notion, Eps8 colocalized with filamentous actin both in immature and lipopolysaccharide (LPS)-matured DCs. Eps8 was prominently localized to

podosomes in immature BMDCs, whereas it was enriched at lamellipodia leading edge of migratory and polarized mature BMDC (Figures S1C and S1D). Genetic removal of *Eps8* did not affect the formation or the number of podosomes, or their ability to adhere or degrade the extracellular matrix (ECM) (data not shown), but altered the shape of both immature and LPS-stimulated BMDCs (Figures S1C and S1D). *Eps8*$^{-/-}$ BMDCs were significantly rounder than WT cells, whereas podosomes, which are frequently polarized in WT immature BMDC, were distributed uniformly in *Eps8*$^{-/-}$ BMDCs (Figure S1D). Eps8 expression was not regulated during DC maturation by LPS (Figure S2). Consistently, Eps8 was dispensable for DC maturation as witnessed by a similar expression pattern of various cell surface activation markers and cytokines (Figures S2A and S2C), that are upregulated during DC maturation. Thus, Eps8 is the main Eps8L family member expressed in BMDCs and represents an abundant actin regulatory protein that is dispensable for the adhesive and degradative properties of BMDCs, but essential for the acquisition of a polarized and elongated cell shape. These data support the notion that Eps8 might be critical for DC migration.

To test this possibility, we analyzed DC migration in response to epicutaneous challenge with a skin irritant that promotes their migration to draining lymph nodes (DLNs) (Akiba et al., 2002). This process is crucial to mount skin immunity (Itano et al., 2003; Sullivan et al., 1986). We, therefore, tested the importance of Eps8 in this very first migratory phase by combining the administration of fluorescein iso-thiocyanate (FITC), which fluorescently labels skin-resident DCs, with the irritant (dibutyl phthalate), which induces DC maturation and mobilization from peripheral, cutaneous tissues to DLNs. We painted the abdomen of WT and *Eps8*$^{-/-}$ mice with FITC and dibutyl phthalate and assessed migration of FITC-positive DCs by flow cytometry (Dearman et al., 1996). The number of dermal DCs (CD24^{-}CD207^{-} and CD24^{-}CD207^{+}) and Langerhans cells (LC; CD24^{+}CD207^{+}) migrating to the DLNs was substantially reduced in *Eps8*$^{-/-}$ as compared to WT mice (Figures 1A and 1B). Notably and as previously reported (Kissenpfennig et al., 2005), the more numerous and faster population of DCs arriving at the DLNs are dermal DCs in both mouse backgrounds. However, in *Eps8*$^{-/-}$ mice dermal DCs were less impaired than LC in their migration as their percentage (relative to migrated FITC^{+} major histocompatibility complex class II [MHCII]$^{+}$ cells) was increased at all time points (Figure 1C), even though their absolute numbers remained lower than in WT mice (Figure 1D, upper panel). Prompted by this result, we also determined the frequency of various DC subtypes under steady state conditions in the skin DLNs as well as in the skin of WT and *Eps8*$^{-/-}$ mice. DLNs from *Eps8*$^{-/-}$ mice displayed a reduced number of all analyzed DC subtypes with respect to WT DLN (Figures S3A–S3C). Conversely, the distribution and number of LCs and dermal DCs determined by immunofluorescence analysis of epidermal sheets and dermal explants, respectively, of WT and *Eps8*$^{-/-}$ mice was nearly identical (Figures S3D and S3E). Collectively, these results indicate that Eps8, which is expressed to various extents in virtually all DC subtypes (Figure S3F), is required for optimal accumulation into DLNs of activated DCs that migrate from the periphery through interstitial tissues, but is not required for the seeding of DC progenitors in the skin.

Delayed-Type Hypersensitivity Is Impaired in *Eps8*$^{-/-}$ Mice Because of DC Migration Deficiency

Because interstitial migration of peripheral DCs is also essential for the priming of CD8^{+} T cells in cutaneous DLNs and mounting of an immunological response (Akiba et al., 2002), we next addressed whether Eps8 is also required for skin immunity by performing a contact hypersensitivity (CHS) assay. WT and *Eps8*$^{-/-}$ mice were sensitized by topical application of oxazolone (OXA) as a hapten (Wang et al., 1997b), and, after 5 days, further challenged by application of the hapten onto the right ear. WT mice responded with a voluminous

swelling of the right ear, whereas the left ear treated with vehicle alone remained normal. In contrast, swelling of the right ears of *Eps8*$^{-/-}$ mice was reduced and OXA-treated ears were nearly indistinguishable from vehicle-treated ears or ears prior to OXA application (Figure 2A). Histological analysis further confirmed that the swelling of WT, but not of *Eps8*$^{-/-}$ mice ears was accompanied by a massive cellular infiltration and edema (Figure 2B).

To assess whether the defect in DC migration observed in *Eps8*$^{-/-}$ mice was cell autonomous or due to lack of Eps8 expression in other tissue compartments, we performed two sets of experiments. In the first set, we tested the delayed-type hypersensitivity (DTH) response after injection of ovalbumin (OVA)-loaded *Eps8*$^{-/-}$ DCs into WT mice and vice versa (WT DCs injected into *Eps8*$^{-/-}$ mice). The adoptive transfer of WT DCs into *Eps8*$^{-/-}$ mice restored the DTH response, which, however, remained significantly impaired in WT mice injected with OVA-pulsed *Eps8*$^{-/-}$ DCs (Figure 2C). Next, we compared the migratory properties of WT and *Eps8*$^{-/-}$ BMDCs injected subcutaneously in WT mice. LPS-matured BMDCs were labeled with two distinct fluorescent dyes and simultaneously injected into the footpad of C57BL/6 mice. Their migration to the popliteal DLN was monitored 1 day after transfer. We found a robust and highly significant decrease in the migration of Eps8-deficient BMDCs to the DLN compared with WT BMDCs (Figure 3A). Similar to WT DCs, the few *Eps8*$^{-/-}$ DCs that reached the DLN localized to the T cell area and were not retained anywhere else in the LN (Figure 3A). These data reinforce the notion that cell-autonomous, migratory defects of DCs, and not Eps8 deficiency in other immune or nonimmune cells, are primarily responsible for the lack of CHS and DTH responses.

Impaired Migration of *Eps8*$^{-/-}$ BMDCs Results in Defective T Cell Priming In Vivo

Next, we determined whether genetic removal of *Eps8*, in addition to preventing migration of antigen-loaded BMDCs to the DLN, also affected the subsequent activation of T cells. We adoptively transferred carboxyfluorescein diacetate succinimidyl ester (CFSE)-labeled CD4$^+$ naive OT-II Ly 5.2 T cells, derived from transgenic mice expressing a T cell receptor (TCR) that specifically recognizes an OVA peptide ($OVA_{323–337}$) in association with MHC class II molecules (Barnden et al., 1998), to C57BL/6 Ly 5.1 mice. After 1 day, mice were injected into the footpad with matured WT or *Eps8*$^{-/-}$ BMDCs and loaded in vitro with OVA; we evaluated T cell proliferation by monitoring CSFE dilution of CD4$^+$ Ly 5.2 T cells isolated from popliteal DLNs. The total number and the proliferation of Ly 5.2 CD4$^+$ T cells were significantly lower after immunization with OVA-loaded *Eps8*$^{-/-}$ BMDCs with respect to OVA-loaded WT BMDCs (Figure 3B). This was not due to defects in antigen uptake or processing by *Eps8*$^{-/-}$ BMDCs (Figures S4A and S4B). Moreover, it could not be accounted for by defects in the ability of OVA-loaded *Eps8*$^{-/-}$ and WT BMDCs to induce antigen-specific T cell proliferation and polarization (secretion of interleukin-2 [IL-2] and interferon-γ [IFN-γ]) in vitro (Figures S4C and S4D). This latter notion was reinforced and validated by two additional approaches. First, we monitored T cell activation and polarization by WT and *Eps8*$^{-/-}$ DCs in round- or flat-bottom wells. In round-bottom wells, contacts between cells are forced by the geometry of the well. Conversely in flat wells, the motility and membrane protrusions activity of DCs is critical to enable their contact and priming of T cells (Benvenuti et al., 2004; Pulecio et al., 2008). *Eps8*$^{-/-}$ DCs promoted T cell proliferation and activation similarly to WT DCs in round, but not in flat-bottom wells (Figure S5A). Under optimal conditions, T cell polarization induced by either WT or *Eps8*$^{-/-}$ DCs was also indistinguishable as attested by a similar pattern of released cytokines (Figure S5B). Second, we tested the priming of adoptively transferred, transgenic CFSE-labeled CD4$^+$ naive OT-II Ly 5.2 T cells by a large amount of OVA-loaded *Eps8*$^{-/-}$ BMDCs injected into the footpad of C57BL/6 Ly 5.1 mice. Under these conditions, larger number of *Eps8*$^{-/-}$ BMDCs reached the DLN (Figure S5C) and induced T cell proliferation to similar extent as OVA-loaded WT BMDCs (Figure S5C).

Thus, Eps8 deficiency does not directly affect DC antigen processing or presentation; rather, it results in a cell-autonomous defect in cell trafficking, which impairs DC migration and ultimately causes defective T cell priming.

Eps8 Removal Impairs Chemotactic BMDCs Motility in 2D and 3D In Vitro

To investigate the cellular and molecular mechanisms underlying Eps8 effects on DC migration, we performed a battery of in vitro migratory assays. We initially tested the chemotactic migratory ability of mature WT and *Eps8*$^{-/-}$ BMDCs in Transwell assays. LPS-stimulated *Eps8*$^{-/-}$ BMDCs were significantly impaired in CCL19-chemotactic migration both under conditions in which no ECM was added to the Transwell (Figure S6A) or when a Matrigel invasion chamber were used (Figure S6B), mimicking 2D and 3D cell motility, respectively. In the latter case, both the total number of cells crossing the invasion chamber and the number of CSFE-stained *Eps8*$^{-/-}$ BMDCs visualized in the process of invading a section of the Matrigel plug were significantly reduced compared with WT BMDCs (Figure S6B). The apparent migratory defect of *Eps8*$^{-/-}$ BMDCs may reflect either a lack of response to chemotactic signals or an intrinsic defective ability of these cells to sustain directional motility, possibly as a consequence of defects of the actin cytoskeletal network supporting cell locomotion. The latter possibility was supported by the observations that *Eps8* null BMDCs were also impaired in Transwell migration under conditions where no chemokine was added to the bottom chamber (data not shown).

To gain further clues in this direction, we monitored BMDC motility in under-agarose assays where cells are squeezed between a layer of agarose and a coverslip. This constrained environment mimics the motility in 3D while affording real-time analysis of individual cell locomotion as well as quantitative measurements of various parameters of cell motility and cell protrusions dynamics (Heit and Kubes, 2003). Mature WT and *Eps8*$^{-/-}$ BMDCs were either exposed to a diffusion gradient of CCL19 or uniformly stimulated with the inclusion of CCL19 in the agarose layer. Tracking of individual cell motility revealed that Eps8 null cells had a significant reduced CCL19 forward migration index, a measure of persistent motility toward a chemotactic stimuli, accompanied by a slight, albeit not significant, reduction of cell speed (Figure 4A and Movie S1). Remarkably, this defect was not limited to cells moving along a diffusive gradient, given that directional persistence (and speed of *Eps8*$^{-/-}$ BMDCs) was significantly reduced also when random cell motility was analyzed (Figure 4B and Movie S2). Thus, Eps8 removal does not strictly impair CCL19 sensing or chemotactic signaling pathways but is more generally required for persistent directional motility of DCs. The finding that CCL19-stimulated and unstimulated, mature WT and Eps8-deficient BMDCs display similar amounts of GTP-bound, activated Rac as well as of a number of signaling kinases (AKT, Erk1, Erk2, and JNK) (Figures S7C and S7D) is consistent with the former notion.

Next, we analyzed WT and *Eps8*$^{-/-}$ BMDC motility in a 3D collagen type I gel because 3D migration substrate that more closely resembles the complex fibrillar environment of dermal interstitial tissues. Collagen type I gels containing CCL19 were polymerized into a homemade chamber on a glass coverslip (Friedl and Bröcker, 2004). On one side of the chamber, WT or *Eps8*$^{-/-}$ BMDCs were added before sealing the chambers for video microscopy analysis. WT BMDCs entered efficiently into the gel moving directionally (directionality index, ~0.53) at ~2 μm/min average velocity. In contrast, *Eps8*$^{-/-}$ BMDCs were significantly slower (average velocity, ~1 μm/min), and displayed a significantly reduced persistent motility (directionality index, ~0.2) (Figure 5 and Movie S3). Thus, removal of Eps8 severely impairs the ability of BMDCs to move in a geometrically defined 3D environment fully recapitulating the severe migration defect observed in vivo.

A corollary prediction of this latter hypothesis is that *Eps8*$^{-/-}$ BMDCs moving in a confined 3D environment may be specifically defective in either the formation or maintenance of cell protrusions, the first step of cell locomotion. To verify this prediction, we embedded BMDCs in collagen scaffolds before exposure to CCL19 and visualized migrating cells at high magnification and resolution to monitor cell protrusion dynamics. Although WT BMDCs extended long protrusions that led the way to cell translocation toward CCL19, more than 80% of *Eps8*$^{-/-}$ BMDCs displayed a round, unpolarized morphology, tumbled around, and failed to effectively translocate their center of mass (Figure 6A, Movie S4). To exemplify and simplify the analysis of the morphological changes and protrusion extension during 3D migration, we traced the cell contour of maximal 3D projection over 5 min of cell translocation (Figure 6B, Movie S4). WT cells frequently extended a persistent protrusion that imposed a polarized morphology with clearly discernible advancing and trailing edges. Conversely, *Eps8*$^{-/-}$ BMDCs formed short-lived protrusions and did not adopt a polarized morphology (Figure 6B). Importantly, *Eps8*$^{-/-}$ BMDCs altered morphological changes and protrusion dynamics could be fully restored by re-expression a wild-type, full-length, GFP-tagged Eps8, formally demonstrating the requirement of Eps8 for BMDC migration morphology (Figure 6C, upper panels, and Movie S5).

The Capping Activity of Eps8 Is Required for Chemotactic BMDC Motility in 3D

We next addressed which of the actin regulatory activities of Eps8 were necessary to restore BMDCs motility. Eps8 possesses both actin capping and bundling activities (Disanza et al., 2004;Disanza et al., 2006). We recently characterized the structural domains responsible for these Eps8 activities: an amphipathic helix (H1), which blocks the barbed end of the filament is responsible for the capping activity, while a compact, globular domain (H2–H5) binds, instead, to the side of filaments and promotes bundling (Hertzog et al., 2010). Eps8 mutants devoid of either capping (Eps8ΔCapping) or bundling (Eps8ΔBundling) activities or both activities (Eps8ΔCapΔBund) could be generated by single-point mutagenesis, thus allowing dissection of their functional roles (Hertzog et al., 2010). We reintroduced these mutants into *Eps8*$^{-/-}$ BMDCs and analyzed their mode of motility in a 3D collagen gel. Although a bundling-deficient mutant was fully capable of restoring cell polarity and protrusion extension to such an extent that cells became undistinguishable from WT BMDCs, the capping and double deficient mutants failed to do so (Figure 6C and Movie S5). We conclude that Eps8 capping activity is essential for BMDCs polarized cell shape and protrusion extension in 3D microenvironment.

Proper Structural Organization and Dynamics of the Lamellipodial Actin Meshwork Requires Eps8

The essential requirement of capping proteins for actin-based motility has been well established through the use of in vitro biomimetic motility assays (Bernheim-Groswasser et al., 2002; Loisel et al., 1999). These results have also been corroborated by in vivo experiments that support a role of cappers in participating in the construction of lamellipodia actin networks in various organisms and model systems (Eddy et al., 1997; Iwasa and Mullins, 2007; Mejillano et al., 2004). Indeed, genetic or functional interference with the activity of the capping protein (CP), the most widely expressed capper, causes loss of the lamellipodia actin meshwork and altered cell protrusion dynamics (Iwasa and Mullins, 2007; Mejillano et al., 2004). At the molecular level, capping proteins have been proposed to work in concert with the Arp2/3 and actin nucleation promoting complexes by blocking barbed ends that are densely packed along leading edges, and thus locally enhancing the availability of monomeric actin that become incorporated into Arp2/3 nuclei (Akin and Mullins, 2008). This may result in increased nucleation events and changes in the architecture of actin networks. To address whether removal of Eps8 leads to similar dynamic and structural alterations in BMDC protrusions and the actin meshwork, we analyzed actin density in

BMDC lamellipodia by platinum replica electron microscopy (EM) and measured protrusion rates and dynamics of WT and *Eps8*$^{-/-}$ BMDCs. The lamellipodia actin meshwork of BMDC displays architecture not dissimilar from other cell types, with an array of actin filaments variably oriented with respect to the leading cellular edges. Notably, however, actin filaments tangentially oriented relative to the leading edge frequently dominated over the orthogonally and diagonally oriented filaments typical for other cells (Koestler et al., 2008; Maly and Borisy, 2001; Svitkina and Borisy, 1999). Remarkably, the actin network of *Eps8*$^{-/-}$ BMDCs' lamellipodia appeared obviously sparser when compared to that of WT lamellipodia (Figure 7A). Quantification of filament density revealed that the actin network in *Eps8*$^{-/-}$ BMDCs was significantly less dense than in WT BMDCs (Figure 7A), whereas no major difference in filament orientation was observed between WT and *Eps8*$^{-/-}$ cells (data not shown). Because the geometry and stiffness of the actin meshwork have been shown to control protrusion persistence and dynamics (Bear et al., 2002; Mogilner and Oster, 2003), we directly measured these parameters by kymograph analysis of BMDCs moving toward CCL19. Although the rate of protrusion extension was nearly identical between WT and *Eps8*$^{-/-}$ BMDCs, removal of *Eps8* caused a significant reduction in protrusion persistence and length, resulting in the formation of much shorter and shorter-lived lamellipodia (Figures 7B and 7C and Movie S6). Similar results were obtained by monitoring with a phase contrast microscope protrusion dynamics of untransfected BMDCs (Figures S7A and S7B). The observation that retrograde actin flow is virtually absent under conditions where integrin-mediated attachment is functional, such as the one we used (Lämmermann et al., 2008; Renkawitz et al., 2009), further suggests that removal of *Eps8* does not affect actin polymerization (the sum of protrusion rate and retrograde actin flow). Instead, Eps8 removal appears to impinge mainly on the architectural organization of the meshwork, which is sparser, and presumably less stiff, and as such is unable to support counter forces that oppose the elongation by polymerization of the actin network.

DISCUSSION

The molecular mechanisms enabling DCs to adapt their actin polymerization rates as well as the architectural organization and rigidity of the actin meshwork that are needed to support cellular deformation-driven locomotion have remained largely elusive. Here, we have shown that Eps8, through its capping activity, is a critical, cell-intrinsic, actin regulatory factor fundamental for DC migration within interstitial tissues in vivo and in vitro. Genetic removal of *Eps8* specifically impairs cell locomotory activity of DC while leaving unaltered a number of other actin-dependent properties of these cells, including integrin-mediated adhesion, matrix degradation, and podosome formation, as well as immunological functions, such as cytokine secretion, antigen presentation, activation and priming of T cells, and cell survival (data not shown). These latter results are relevant because they argue that the function of Eps8 in DCs is to directly control the dynamics and architectural organization of the actin meshwork, rather than to participate in the transduction of signals leading to Racdependent actin remodeling as in fibroblasts (Scita et al., 1999).

The most striking cellular defects of *Eps8* null BMDCs is their inability to extend persistent and elongated protrusions in a 3D matrix, under conditions in which the rate of extension of individual cell protrusion is similar to that of WT DC. This altered protrusion dynamics prevents *Eps8* null BMDCs from adopting a defined front-to-back polarity and from extending pseudopodia into fluid-filled gaps of fibrillar collagen, thus driving forward movement. The net results is that *Eps8*$^{-/-}$ DCs, instead of moving directionally, tumble around emitting short-lived, nondirectional cell protrusions that fail to drive effective cell locomotion. This in vitro finding is likely to explain the impaired DC migration observed in murine interstitial tissues. Notably, in 2D or in under-agarose migratory setting, removal of *Eps8* has more limited effects on BMDC velocity, although it significantly impaired

directional migration and chemotactic movement. A similar specific defective migration in 3D, but not in 2D, of DCs has also recently been reported after the removal of Cdc42, a small RhoGTPase critically controlling polarized migration (Lämmermann et al., 2009). As with Eps8 deficient BMDCs, *Cdc42*$^{-/-}$ cells are unable to migrate both in mice and in in vitro 3D motility systems, whereas they display limited defects in a 2D setting (Lämmermann et al., 2009). However, there are obvious differences with respect to the phenotype of *Eps8*$^{-/-}$ cells. *Cdc42* null BMDC extend multiple protrusions, but that are spatially and temporally deregulated, leading to impaired coordination between actin flow and the leading edge. This enables cells to move in 2D or under agarose in response to chemotactic signals at almost the same speed as WT cells and with limited directional defects, but causes arrest of migration in 3D. In collagen type I gels, *Cdc42*$^{-/-}$ DCs form multiple competing protrusions that cause instantaneous entanglement of the cells within 3D ECM fibers (Lämmermann et al., 2009). Conversely, *Eps8* null BMDCs are not stuck by entanglement but affected in their ability to extend persistent protrusions particularly in a 3D microenvironment. The presumably less rigid actin meshwork of *Eps8*$^{-/-}$ BMDCs is unable to support the increased resistance generated by the geometrically constrained 3D fibrillar matrix, resulting in cells that fail to polarize along the direction determined by long-lived pseudopodia. EM analysis of the actin meshwork, which is significantly less dense in *Eps8*$^{-/-}$ BMDCs, supports this contention. The extension and dynamics of pseudopodia can be restored by re-expression of a WT *Eps8* or a bundling-deficient mutant, but not by a capping-deficient mutant, pointing to a critical requirement of this activity for directional motility and 3D BMDC migration. Similar alterations in protrusion dynamics have been reported in mesenchymal cells in which capping activity is suppressed by RNAi against CP or by forced expression of VASP, a multifunctional actin regulator that can also exert anticapping function (Bear et al., 2002; Mejillano et al., 2004). Thus, one major impact of altering capping activity may be to change the architecture and movement of the actin network underlying cell protrusions. It is noteworthy that similar conclusions as to the role of capping in actin motility have also been reached recently with in vitro-reconstituted, biomimetic motility systems (Akin and Mullins, 2008). According to this study, capping proteins appear to work in concert with the Arp2/3 complex to control the rate of nucleation (Akin and Mullins, 2008). This impacts on the architectural organization of the actin meshwork, whose stiffness and rigidity may, in turn, influence protrusion dynamics and cell motility, particularly in microenvironments characterized by an increased resistance-load against advancing leading edges, such as in 3D intestinal tissues.

Why *Eps8* removal leads to such dramatic alterations in cells that express also other capping proteins, including CP (data not shown), is not entirely clear. The unique properties of Eps8 among cappers may account for this: Eps8 regulation is determined by protein:protein interactions (Disanza et al., 2004) as well as mitogen-activated protein kinase (MAPK)-dependent posttranslational phosphorylation (Menna et al., 2009). Within this context, it is noteworthy that the chemokine CCL19 binding to its receptor (CCR7) has been shown to activate two signaling axes relevant for migration: a Rho-Pyk-cofilin axis that regulates the velocity of DC locomotion and MAPK and Jun-N-terminal kinase (JNK) cascades that impact on chemotaxis (Riol-Blanco et al., 2005). Whether Eps8 is the final actin regulatory target of the latter pathway has not been tested, but represents an interesting possibility for future investigation.

What is the immunological outcome of *Eps8* deficiency? *Eps8* null mice do not mount a CHS response. This is paralleled by the inability of Eps8-deficient DCs to migrate to DLNs in response to a skin irritant, or to initiate antigen-specific T cell responses. This is not due to the inability of DCs to process or present antigens, but just to migrate toward T cells. Because Eps8 is not expressed in T cells and is not required for the phenotypical and functional maturation of DCs, in its absence, impairment of induction of immunity in vivo is

owed primarily to the incapacity of DCs to reach DLNs for T cell activation. Hence, differently from other actin-binding proteins such as mDia1 and WASP that are involved in several other properties of DCs (Bouma et al., 2007; Bouma et al., 2009; Burns et al., 2001; Calle et al., 2004; Monypenny et al., 2010; Tanizaki et al., 2010), Eps8 has a unique activity solely in DC migration. Indirectly, our results indicate also that DC migration from the site of inflammation is necessary for the induction of immunity because DCs that are still capable of driving T cell responses, but unable to reach the DLN, cannot initiate immune responses.

Together, these results point to a unique and nonredundant role of Eps8 in the polarized migration of DCs. Given the recognized ability of pathogens, primarily viruses, to interfere with the antigen-processing machinery as well as the migratory property of DCs (Lambotin et al., 2010; Theodoridis et al., 2011), it would be interesting to address in future studies whether also the actin capping activity of Eps8 could be a target of immune escape mechanisms.

Supplementary Material

Refer to Web version on PubMed Central for supplementary material.

Acknowledgments

We thank M. Sixt for sharing protocols and for discussion, A. Prescot for initial technical support on DC imaging, and R. Gunby for critically reading and editing the manuscript. This work was supported by grants from the Associazione Italiana per la Ricerca sul Cancro (AIRC) to G.S., A.D. and M.R; the Italian Ministries of Education-University-Research (MIUR-PRIN) and of Health to G.S.; the AICR (International Association For Cancer Research -AICR) to G.S. and M.R.; the CARIPLO Foundations to G.S. and M.R.; and the European Research Council to M.R. and G.S.

REFERENCES

Abbott MA, Wells DG, Fallon JR. The insulin receptor tyrosine kinase substrate p58/53 and the insulin receptor are components of CNS synapses. J. Neurosci. 1999; 19:7300–7308. [PubMed: 10460236]

Akiba H, Kehren J, Ducluzeau MT, Krasteva M, Horand F, Kaiserlian D, Kaneko F, Nicolas JF. Skin inflammation during contact hypersensitivity is mediated by early recruitment of CD8+ T cytotoxic 1 cells inducing keratinocyte apoptosis. J. Immunol. 2002; 168:3079–3087. [PubMed: 11884482]

Akin O, Mullins RD. Capping protein increases the rate of actin-based motility by promoting filament nucleation by the Arp2/3 complex. Cell. 2008; 133:841–851. [PubMed: 18510928]

Barnden MJ, Allison J, Heath WR, Carbone FR. Defective TCR expression in transgenic mice constructed using cDNA-based alpha-and beta-chain genes under the control of heterologous regulatory elements. Immunol. Cell Biol. 1998; 76:34–40. [PubMed: 9553774]

Bear JE, Svitkina TM, Krause M, Schafer DA, Loureiro JJ, Strasser GA, Maly IV, Chaga OY, Cooper JA, Borisy GG, Gertler FB. Antagonism between Ena/VASP proteins and actin filament capping regulates fibroblast motility. Cell. 2002; 109:509–521. [PubMed: 12086607]

Benvenuti F, Hugues S, Walmsley M, Ruf S, Fetler L, Popoff M, Tybulewicz VL, Amigorena S. Requirement of Rac1 and Rac2 expression by mature dendritic cells for T cell priming. Science. 2004; 305:1150–1153. [PubMed: 15326354]

Bernheim-Groswasser A, Wiesner S, Golsteyn RM, Carlier MF, Sykes C. The dynamics of actin-based motility depend on surface parameters. Nature. 2002; 417:308–311. [PubMed: 12015607]

Bouma G, Burns S, Thrasher AJ. Impaired T-cell priming in vivo resulting from dysfunction of WASp-deficient dendritic cells. Blood. 2007; 110:4278–4284. [PubMed: 17673604]

Bouma G, Burns SO, Thrasher AJ. Wiskott-Aldrich Syndrome: Immunodeficiency resulting from defective cell migration and impaired immunostimulatory activation. Immunobiology. 2009; 214:778–790. [PubMed: 19628299]

Burns S, Thrasher AJ, Blundell MP, Machesky L, Jones GE. Configuration of human dendritic cell cytoskeleton by Rho GTPases, the WAS protein, and differentiation. Blood. 2001; 98:1142–1149. [PubMed: 11493463]

Calle Y, Chou HC, Thrasher AJ, Jones GE. Wiskott-Aldrich syndrome protein and the cytoskeletal dynamics of dendritic cells. J. Pathol. 2004; 204:460–469. [PubMed: 15495215]

Croce A, Cassata G, Disanza A, Gagliani MC, Tacchetti C, Malabarba MG, Carlier MF, Scita G, Baumeister R, Di Fiore PP. A novel actin barbed-end-capping activity in EPS-8 regulates apical morphogenesis in intestinal cells of Caenorhabditis elegans. Nat. Cell Biol. 2004; 6:1173–1179. [PubMed: 15558032]

Dearman RJ, Cumberbatch M, Hilton J, Clowes HM, Fielding I, Heylings JR, Kimber I. Influence of dibutyl phthalate on dermal sensitization to fluorescein isothiocyanate. Fundam. Appl. Toxicol. 1996; 33:24–30. [PubMed: 8812211]

Disanza A, Carlier MF, Stradal TE, Didry D, Frittoli E, Confalonieri S, Croce A, Wehland J, Di Fiore PP, Scita G. Eps8 controls actin-based motility by capping the barbed ends of actin filaments. Nat. Cell Biol. 2004; 6:1180–1188. [PubMed: 15558031]

Disanza A, Mantoani S, Hertzog M, Gerboth S, Frittoli E, Steffen A, Berhoerster K, Kreienkamp HJ, Milanesi F, Di Fiore PP, et al. Regulation of cell shape by Cdc42 is mediated by the synergic actin-bundling activity of the Eps8-IRSp53 complex. Nat. Cell Biol. 2006; 8:1337–1347. [PubMed: 17115031]

Eddy RJ, Han J, Condeelis JS. Capping protein terminates but does not initiate chemoattractant-induced actin assembly in Dictyostelium. J. Cell Biol. 1997; 139:1243–1253. [PubMed: 9382870]

Friedl P, Bröcker EB. The biology of cell locomotion within three-dimensional extracellular matrix. Cell. Mol. Life Sci. 2000; 57:41–64. [PubMed: 10949580]

Friedl P, Bröcker EB. Reconstructing leukocyte migration in 3D extracellular matrix by time-lapse videomicroscopy and computer-assisted tracking. Methods Mol. Biol. 2004; 239:77–90. [PubMed: 14573911]

Funato Y, Terabayashi T, Suenaga N, Seiki M, Takenawa T, Miki H. IRSp53/Eps8 complex is important for positive regulation of Rac and cancer cell motility/invasiveness. Cancer Res. 2004; 64:5237–5244. [PubMed: 15289329]

Heit B, Kubes P. Measuring chemotaxis and chemokinesis: The under-agarose cell migration assay. Sci. STKE. 2003; 2003:PL5. [PubMed: 12591998]

Hertzog M, Milanesi F, Hazelwood L, Disanza A, Liu H, Perlade E, Malabarba MG, Pasqualato S, Maiolica A, Confalonieri S, et al. Molecular basis for the dual function of Eps8 on actin dynamics: Bundling and capping. PLoS Biol. 2010; 8 e1000387.

Itano AA, McSorley SJ, Reinhardt RL, Ehst BD, Ingulli E, Rudensky AY, Jenkins MK. Distinct dendritic cell populations sequentially present antigen to CD4 T cells and stimulate different aspects of cell-mediated immunity. Immunity. 2003; 19:47–57. [PubMed: 12871638]

Iwasa JH, Mullins RD. Spatial and temporal relationships between actin-filament nucleation, capping, and disassembly. Curr. Biol. 2007; 17:395–406. [PubMed: 17331727]

Kissenpfennig A, Henri S, Dubois B, Laplace-Builhé C, Perrin P, Romani N, Tripp CH, Douillard P, Leserman L, Kaiserlian D, et al. Dynamics and function of Langerhans cells in vivo: Dermal dendritic cells colonize lymph node areas distinct from slower migrating Langerhans cells. Immunity. 2005; 22:643–654. [PubMed: 15894281]

Koestler SA, Auinger S, Vinzenz M, Rottner K, Small JV. Differentially oriented populations of actin filaments generated in lamellipodia collaborate in pushing and pausing at the cell front. Nat. Cell Biol. 2008; 10:306–313. [PubMed: 18278037]

Lambotin M, Baumert TF, Barth H. Distinct intracellular trafficking of hepatitis C virus in myeloid and plasmacytoid dendritic cells. J. Virol. 2010; 84:8964–8969. [PubMed: 20573834]

Lämmermann T, Bader BL, Monkley SJ, Worbs T, Wedlich-Söldner R, Hirsch K, Keller M, Förster R, Critchley DR, Fässler R, Sixt M. Rapid leukocyte migration by integrin-independent flowing and squeezing. Nature. 2008; 453:51–55. [PubMed: 18451854]

Lämmermann T, Renkawitz J, Wu X, Hirsch K, Brakebusch C, Sixt M. Cdc42-dependent leading edge coordination is essential for interstitial dendritic cell migration. Blood. 2009; 113:5703–5710. [PubMed: 19190242]

Lanzetti L, Rybin V, Malabarba MG, Christoforidis S, Scita G, Zerial M, Di Fiore PP. The Eps8 protein coordinates EGF receptor signalling through Rac and trafficking through Rab5. Nature. 2000; 408:374–377. [PubMed: 11099046]

Loisel TP, Boujemaa R, Pantaloni D, Carlier MF. Reconstitution of actin-based motility of Listeria and Shigella using pure proteins. Nature. 1999; 401:613–616. [PubMed: 10524632]

Maly IV, Borisy GG. Self-organization of a propulsive actin network as an evolutionary process. Proc. Natl. Acad. Sci. USA. 2001; 98:11324–11329. [PubMed: 11572984]

Manor U, Disanza A, Grati M, Andrade L, Lin H, Di Fiore PP, Scita G, Kachar B. Regulation of stereocilia length by myosin XVa and whirlin depends on the actin-regulatory protein Eps8. Curr. Biol. 2011; 21:167–172. [PubMed: 21236676]

Mejillano MR, Kojima S, Applewhite DA, Gertler FB, Svitkina TM, Borisy GG. Lamellipodial versus filopodial mode of the actin nanomachinery: Pivotal role of the filament barbed end. Cell. 2004; 118:363–373. [PubMed: 15294161]

Menna E, Disanza A, Cagnoli C, Schenk U, Gelsomino G, Frittoli E, Hertzog M, Offenhauser N, Sawallisch C, Kreienkamp HJ, et al. Eps8 regulates axonal filopodia in hippocampal neurons in response to brain-derived neurotrophic factor (BDNF). PLoS Biol. 2009; 7 e1000138.

Mogilner A, Oster G. Force generation by actin polymerization II: The elastic ratchet and tethered filaments. Biophys. J. 2003; 84:1591–1605. [PubMed: 12609863]

Monypenny J, Chou HC, Banon-Rodriguez I, Thrasher AJ, Anton IM, Jones GE, Calle Y. Role of WASP in cell polarity and podosome dynamics of myeloid cells. Eur. J. Cell Biol. 2010; 90:198–204. [PubMed: 20609498]

Oda K, Shiratsuchi T, Nishimori H, Inazawa J, Yoshikawa H, Taketani Y, Nakamura Y, Tokino T. Identification of BAIAP2 (BAI-associated protein 2), a novel human homologue of hamster IRSp53, whose SH3 domain interacts with the cytoplasmicdomain of BAI1. Cytogenet. Cell Genet. 1999; 84:75–82. [PubMed: 10343108]

Offenhäuser N, Borgonovo A, Disanza A, Romano P, Ponzanelli I, Iannolo G, Di Fiore PP, Scita G. The eps8 family of proteins links growth factor stimulation to actin reorganization generating functional redundancy in the Ras/Rac pathway. Mol. Biol. Cell. 2004; 15:91–98. [PubMed: 14565974]

Pierre P, Turley SJ, Gatti E, Hull M, Meltzer J, Mirza A, Inaba K, Steinman RM, Mellman I. Developmental regulation of MHC class II transport in mouse dendritic cells. Nature. 1997; 388:787–792. [PubMed: 9285592]

Pulecio J, Tagliani E, Scholer A, Prete F, Fetler L, Burrone OR, Benvenuti F. Expression of Wiskott-Aldrich syndrome protein in dendritic cells regulates synapse formation and activation of naive CD8+ T cells. J. Immunol. 2008; 181:1135–1142. [PubMed: 18606666]

Randolph GJ, Ochando J, Partida-Sánchez S. Migration of dendritic cell subsets and their precursors. Annu. Rev. Immunol. 2008; 26:293–316. [PubMed: 18045026]

Renkawitz J, Schumann K, Weber M, Lämmermann T, Pflicke H, Piel M, Polleux J, Spatz JP, Sixt M. Adaptive force transmission in amoeboid cell migration. Nat. Cell Biol. 2009; 11:1438–1443. [PubMed: 19915557]

Riol-Blanco L, Sánchez-Sánchez N, Torres A, Tejedor A, Narumiya S, Corbí AL, Sánchez-Mateos P, Rodríguez-Fernández JL. The chemokine receptor CCR7 activates in dendritic cells two signaling modules that independently regulate chemotaxis and migratory speed. J. Immunol. 2005; 174:4070–4080. [PubMed: 15778365]

Scita G, Nordstrom J, Carbone R, Tenca P, Giardina G, Gutkind S, Bjarnegård M, Betsholtz C, Di Fiore PP. EPS8 and E3B1 transduce signals from Ras to Rac. Nature. 1999; 401:290–293. [PubMed: 10499589]

Sullivan S, Bergstresser PR, Tigelaar RE, Streilein JW. Induction and regulation of contact hypersensitivity by resident, bone marrow-derived, dendritic epidermal cells: Langerhans cells and Thy-1+ epidermal cells. J. Immunol. 1986; 137:2460–2467. [PubMed: 2876041]

Svitkina TM, Borisy GG. Correlative light and electron microscopy of the cytoskeleton of cultured cells. Methods Enzymol. 1998; 298:570–592. [PubMed: 9751908]

Svitkina TM, Borisy GG. Progress in protrusion: The tell-tale scar. Trends Biochem. Sci. 1999; 24:432–436. [PubMed: 10542409]

Tanizaki H, Egawa G, Inaba K, Honda T, Nakajima S, Moniaga CS, Otsuka A, Ishizaki T, Tomura M, Watanabe T, et al. Rho-mDia1 pathway is required for adhesion, migration, and T-cell stimulation in dendritic cells. Blood. 2010; 116:5875–5884. [PubMed: 20881208]

Theodoridis AA, Eich C, Figdor CG, Steinkasserer A. Infection of dendritic cells with herpes simplex virus type 1 induces rapid degradation of CYTIP, thereby modulating adhesion and migration. Blood. 2011; 118:107–115. [PubMed: 21562043]

Tocchetti A, Confalonieri S, Scita G, Di Fiore PP, Betsholtz C. In silico analysis of the EPS8 gene family: genomic organization, expression profile, and protein structure. Genomics. 2003; 81:234–244. [PubMed: 12620401]

Tocchetti A, Soppo CB, Zani F, Bianchi F, Gagliani MC, Pozzi B, Rozman J, Elvert R, Ehrhardt N, Rathkolb B, et al. Loss of the actin remodeler Eps8 causes intestinal defects and improved metabolic status in mice. PLoS ONE. 2010; 5:e9468. [PubMed: 20209148]

Wang B, Fujisawa H, Zhuang L, Kondo S, Shivji GM, Kim CS, Mak TW, Sauder DN. Depressed Langerhans cell migration and reduced contact hypersensitivity response in mice lacking TNF receptor p75. J. Immunol. 1997a; 159:6148–6155. [PubMed: 9550416]

Wang Y, O'Rourke J, Cone RE. Serum TABM produced during anterior chamber-associated immune deviation passively transfers suppression of delayed-type hypersensitivity to primed mice. Int. Immunol. 1997b; 9:211–218. [PubMed: 9040003]

West MA, Wallin RP, Matthews SP, Svensson HG, Zaru R, Ljunggren HG, Prescott AR, Watts C. Enhanced dendritic cell antigen capture via toll-like receptor-induced actin remodeling. Science. 2004; 305:1153–1157. [PubMed: 15326355]

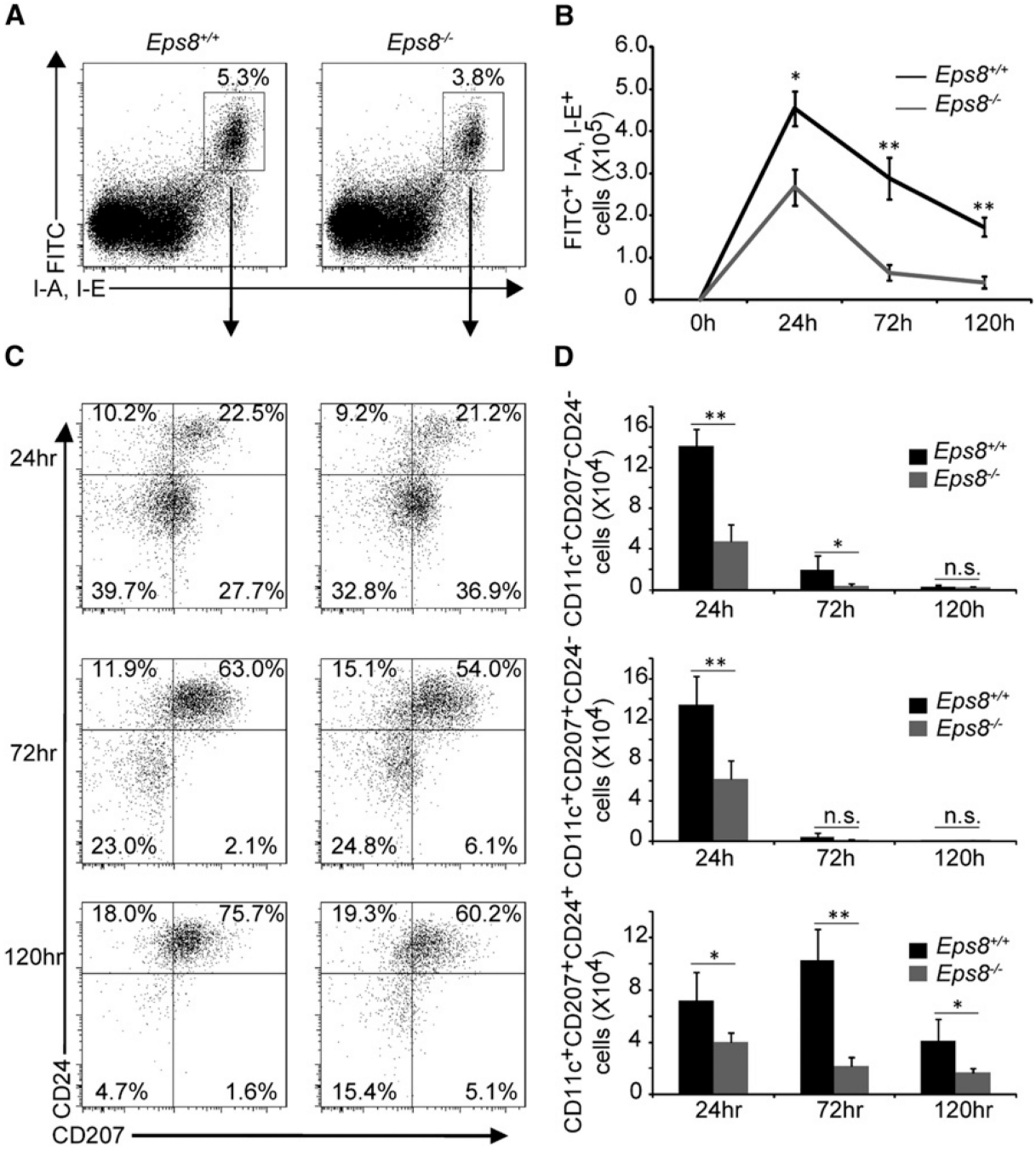

Figure 1. Skin Irritant-Induced DC Migration to Cutaneous DLNs Is Impaired in *Eps8* Null Mice

(A) The percentage of FITC$^+$ MHCII$^+$ skin cells migrating to inguinal DLNs of WT (*Eps8*$^{+/+}$) or *Eps8*$^{-/-}$ (*Eps8*$^{-/-}$) mice painted on the abdomen with 0.5% FITC in 1:1 acetone:dibutylphtalate mixture was assessed by flow cytometry. Numbers in the gate are the percentage of FITC$^+$ MHCII$^+$ positive cells (6 mice/group, two independent experiments).

(B) The absolute numbers of FITC$^+$ MHCII$^+$ CD11c$^+$ cells migrating to the DLNs at different time points in WT (*Eps8*$^{+/+}$) and Eps8-deficient (*Eps8*$^{-/-}$) animals. Data represent the mean ± SD (6 mice/group, out of two independent experiments).

(C)FITC$^+$MHCII$^+$CD11c$^+$ cells were analyzed for the expression of CD24 and CD207. Numbers in the quadrants show the percentage of positive cells.
(D) The absolute numbers of FITC$^+$ dermal DCs (CD24$^-$ CD207$^-$), langerin dermal DCs (CD24$^-$ CD207$^+$) and Langerhans cells (CD24$^+$ CD207$^+$) migrating to the DLNs at different time points in WT (*Eps8*$^{+/+}$) and Eps8-deficient (*Eps8*$^{-/-}$) animals. Data represent the mean ± SD (n = 6 mice/group of two independent experiments); *p < 0.05; **p < 0.01; ***p < 0.001.

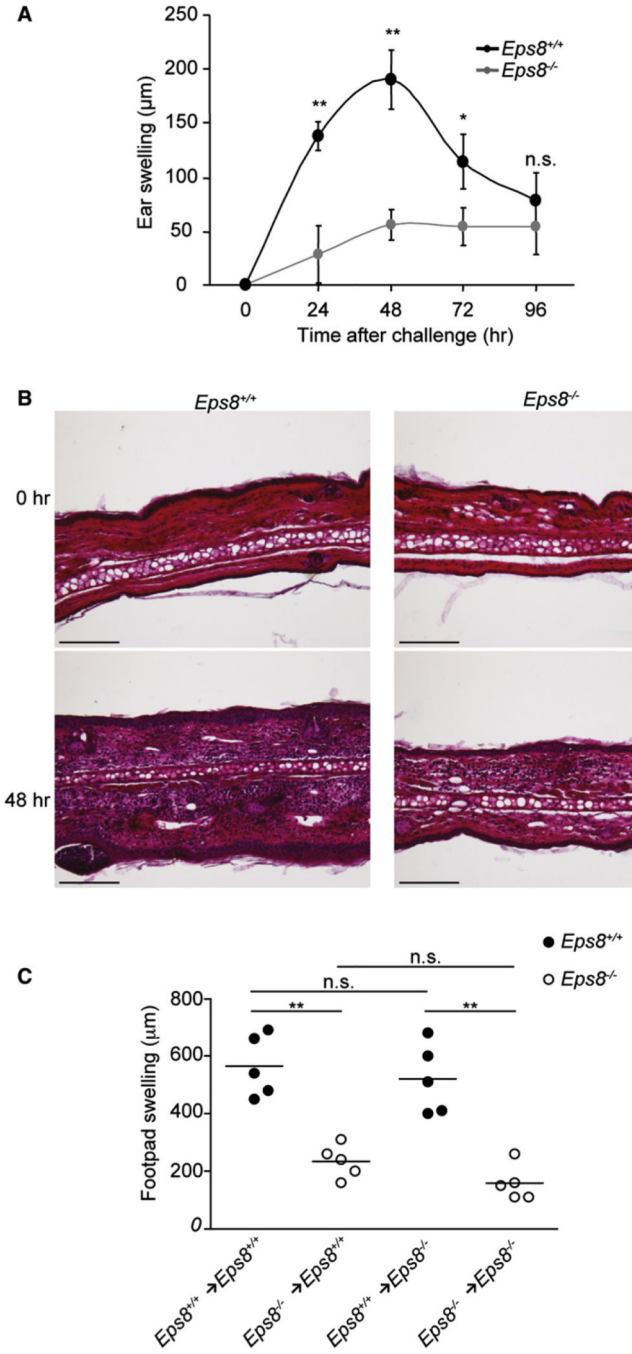

Figure 2. Impaired CHS Response to Oxazolone in the Absence of *Eps8*

(A) *Eps8* deficiency significantly impairs ear swelling upon OXA sensitization. WT ($Eps8^{+/+}$) and $Eps8^{-/-}$ ($Eps8^{-/-}$) mice sensitized with OXA on day 0, were challenged after 5 days on the right ear with OXA. Ear thickness was measured from 24 hr to 96 hr after challenge. Data represent the mean swelling values of 5 mice/group of three independent experiments. **p < 0.01; *p < 0.05.

(B) Cellular infiltrate and edema are reduced in Eps8-deficient mice 48 hr after OXA challenge. Histological analysis of the CHS response: WT ($Eps8^{+/+}$, left panels) and Eps8-deficient ($Eps8^{-/-}$, right panels) mice ears, unchallenged (top) or 48 hr after OXA challenge (bottom). The scale bar represents 200 μm.

(C) WT (*Eps8*$^{+/+}$, black circle) and Eps8-deficient mice (*Eps8*$^{-/-}$, open circle) immunized with WT or Eps8-deficient OVA-loaded BMDCs cells were challenged with OVA in the right footpad and vehicle in the left footpad. Data represent the mean swelling values of 5 mice/group of two independent experiments. **$p < 0.01$; *$p < 0.05$.

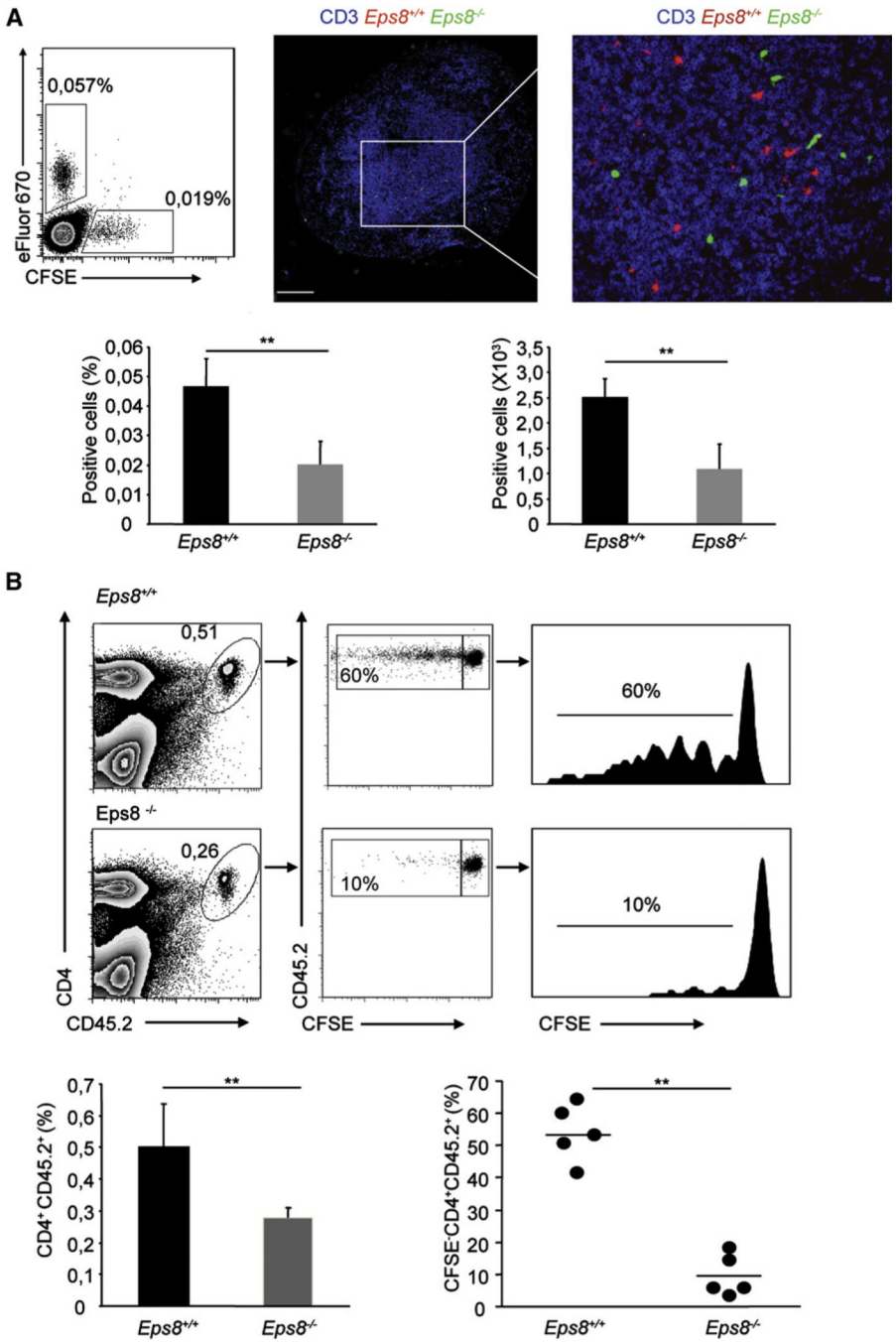

Figure 3. Impaired Trafficking and Antigen Presentation in DLNs of Subcutaneously Injected Eps8-Deficient DCs

(A) Eps8-deficient DCs fail to migrate to DLNs. LPS-treated WT (*Eps8*$^{+/+}$) or *Eps8*$^{-/-}$ (*Eps8*$^{-/-}$) BMDCs were stained with either eFluor670 or CFSE, respectively. An equal number (1.5×10^5) of WT and *Eps8*$^{-/-}$ labeled BMDCs were injected in the footpad. The number of migrated BMDCs to the popliteal DLN was assessed by flow cytometry after 24 hr. The top-left panel is a representative dot plot of three independent experiments. The percentage of eFluor670- or CFSE-positive DLN cells is shown. The top-right panel shows a confocal section of a popliteal DLN after migration of eFluor670-labeled WT (*Eps8*$^{+/+}$), CFSE-labeled *Eps8*$^{-/-}$ (*Eps8*$^{-/-}$) BMDCs, and anti-CD3 staining for visualization of the T

cell area. The scale bar represents 250 μm. Data represent mean ± SD (n = 5 mice). **p < 0.01; *p < 0.05.

(B) *Eps8*$^{-/-}$ DCs fail to migrate to DLNs and to prime naive T cells. C57BL/6 Ly 5.1 mice were adoptively transferred with 2 × 10^6 CFSE-labeled CD4 naive OT-II Ly 5.2 T cells. After 24 hr, mice were injected in the right or in the left footpad with 1.5 × 10^5 WT (*Eps8*$^{+/+}$) or *Eps8*$^{-/-}$ (*Eps8*$^{-/-}$) mature Ova-loaded BMDCs, respectively. The popliteal DLNs were analyzed for assessing the percentage of CD4 Ly 5.2 T cells and the proliferation via CFSE dilution after 3 d. Left panels show the percentage of $CD4^+$ and $CD45.2^+$ positive cells in the DLN is shown. The middle panel shows the percentage of proliferated $CD4^+$ and $CD45.2^+$ T cells. Right panels show histograms of CFSE dilution in $CD4^+CD45.2^+$ T cells. Numbers above lines is the percentages of proliferating cells. Data represent the mean ± SD (n = 5 mice/group) of three independent experiments; **p < 0.01, *p < 0.05.

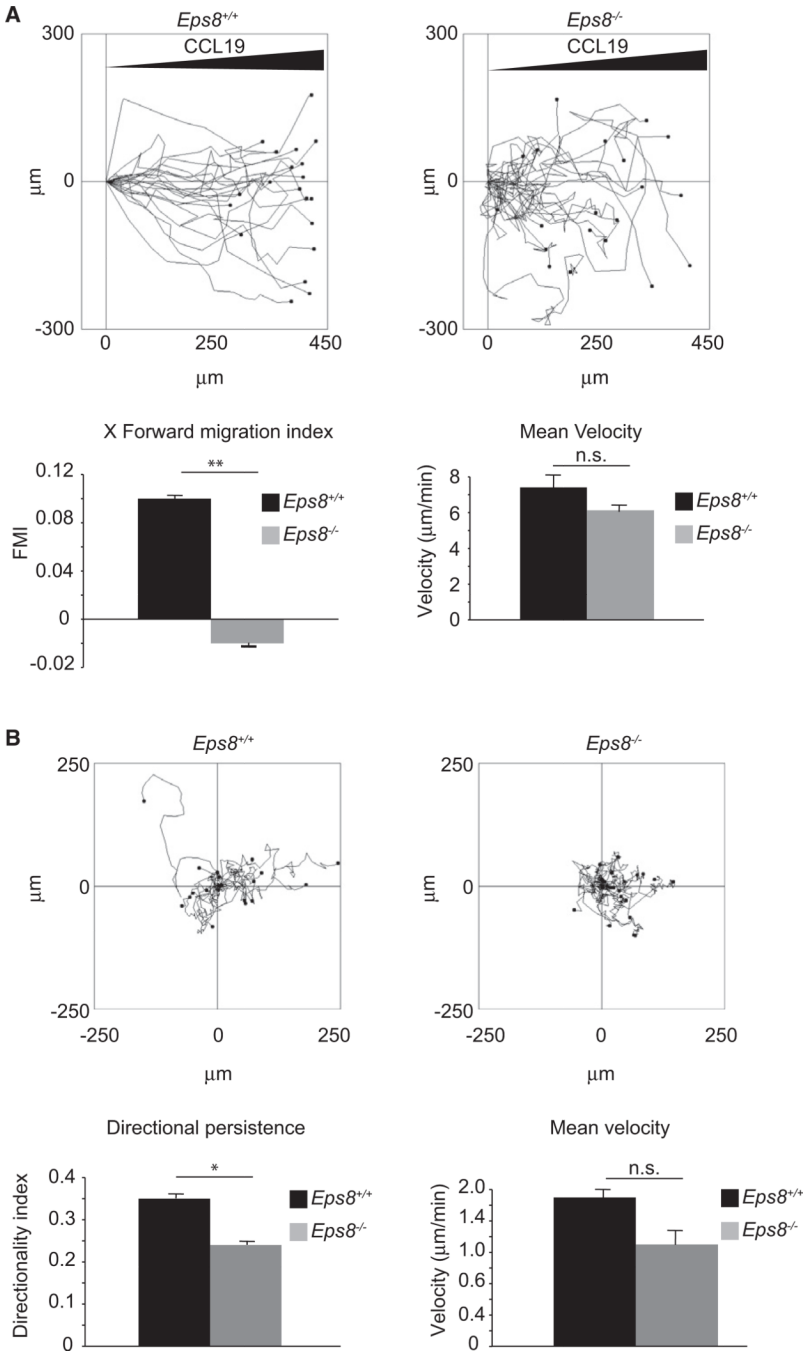

Figure 4. Genetic Removal of *Eps8* Impairs Directional Motility of BMDCs in Under-Agarose Assays

(A) An equal number of LPS-activated WT (*Eps8*$^{+/+}$) and *Eps8*$^{-/-}$ (*Eps8*$^{-/-}$) BMDCs were injected between a glass coverslip and an agarose layer. Cells were induced to migrate toward a 2mm afar attractor hole containing CCL19. Migration tracks of randomly picked cells are shown on the left (see also Movie S1). The forward migration index and mean velocity (right graphs) ± SD are shown. At least 30 single cells /experiment/genotype were tracked. n.s. not significant; **p < 0.01.

(B) Random BMDC migration in a planar under-agarose assay. BMDCs were treated as in (A) and injected between a glass coverslip and a layer of agarose. Data are presented as in

(A) except that the directionality index is reported instead of forward migration index (right graphs). (see also Movie S2). At least 30 single cells/experiment/genotype (three independent BMDC preparations) were tracked. Data are the mean ± SD. n.s. not significant; *$p < 0.05$.

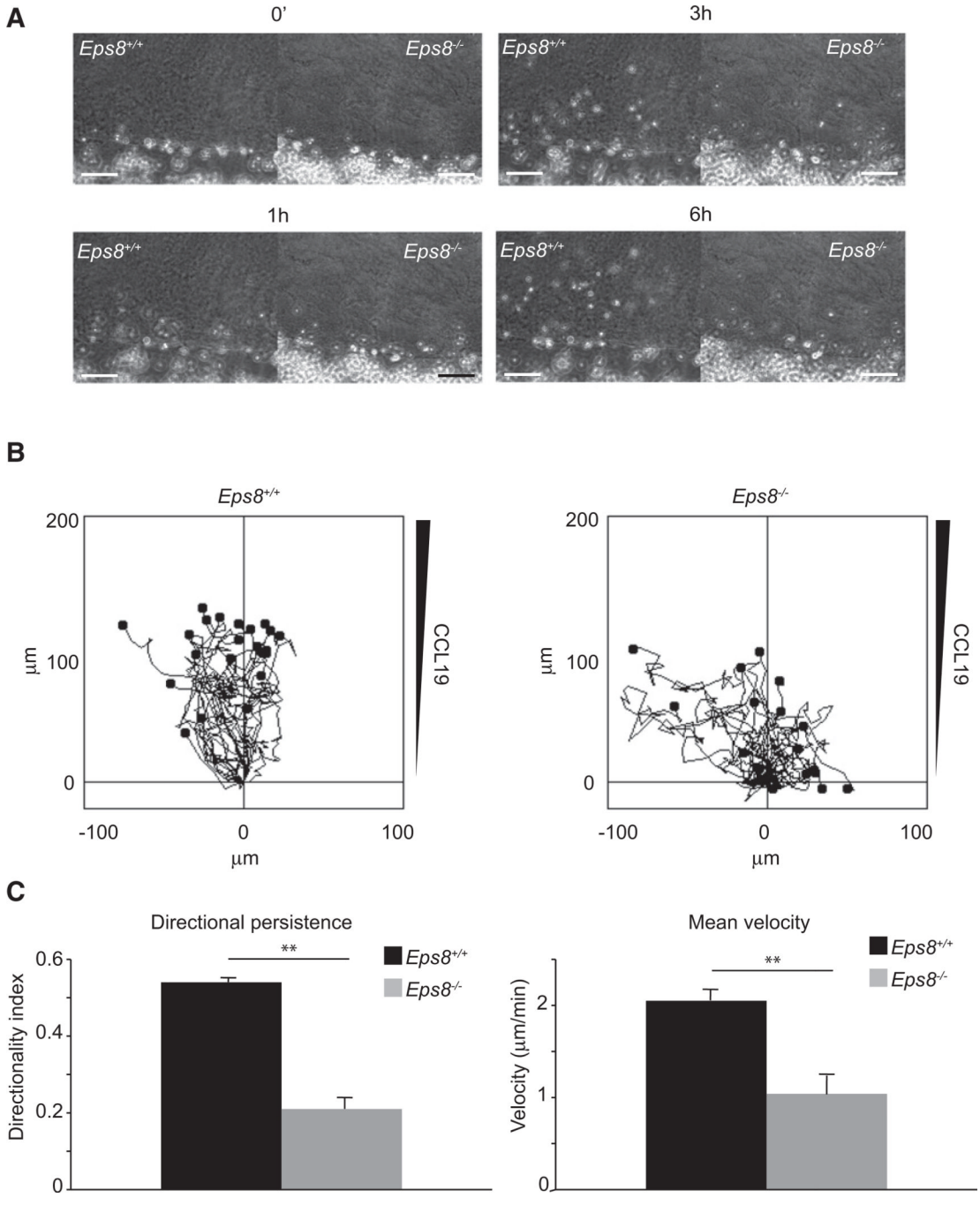

Figure 5. Genetic Removal of *Eps8* Impairs Chemotactic Motility of BMDC in 3D Collage Matrix Chamber Slides

(A) An equal number of LPS-activated WT (*Eps8*$^{+/+}$) and *Eps8*$^{-/-}$ (*Eps8*$^{-/-}$) BMDCs were placed on one side of a chamber slide in which 1.6 mg/ml polymerized collagen type I gel containing 1.2 μg/ml CCL19 was added (Friedl and Bröcker, 2000). A time sequence of migratory WT and *Eps8*$^{-/-}$ BMDCs is shown (see also Movie S3). The scale bar represents 150 μm.

(B and C) Migration tracks of randomly picked individual cells (B). Cell directionality (C, left graph) and mean velocity (C, right graph) were measured. The analysis was conducted

on 35 single cells/experiment/genotype of three independent BMDC preparations; data are the mean ± SD. **p < 0.01.

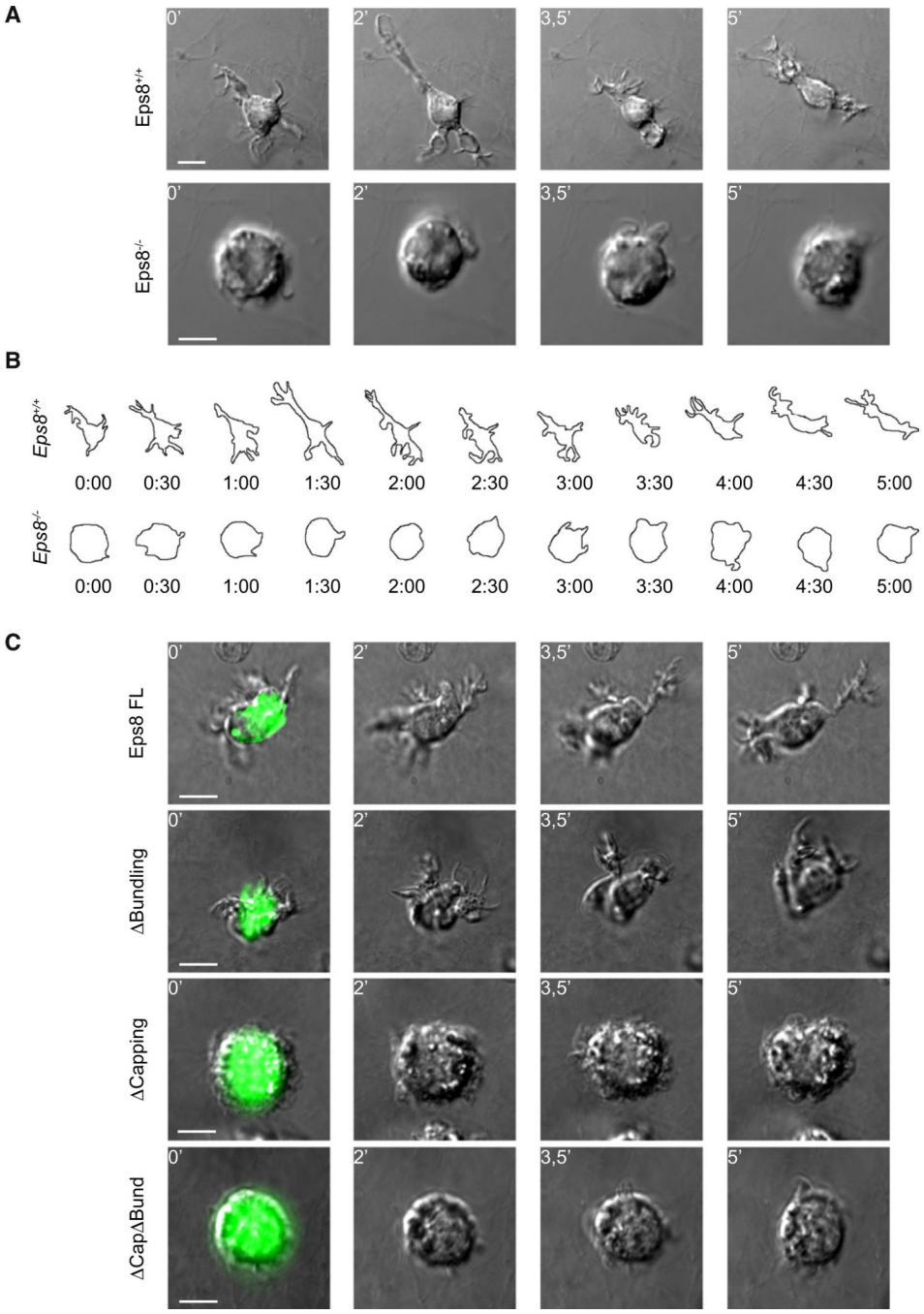

Figure 6. Eps8 Capping Activity Is Required for the Extension of Elongated and Persistent Cell Protrusions of BMDCs in 3D

(A and B) *Eps8*$^{-/-}$ BMDCs fail to extend elongated cell protrusions and to migrate in 3D upon CCL19 stimulation.

(A) LPS-treated WT (*Eps8*$^{+/+}$) and *Eps8*$^{-/-}$ (*Eps8*$^{-/-}$) BMDCs were embedded in 1.6 mg/ml collagen type I chamber slides. CCL19 (1.2 μg/ml) was added to the top of the polymerized matrix before sealing the chamber. BMDC motility was recorded by spinning disk confocal microscopy. Still images from Movie S4 are shown. Scale bars represent 15 μm or 10 μm.

(B) Morphology outlines of WT (*Eps8*$^{+/+}$) and *Eps8*$^{-/-}$ (*Eps8*$^{-/-}$) BMDCs were obtained by morphometric analysis of 3D maximal projections. A time sequence of representative migratory WT (*Eps8*$^{+/+}$) and *Eps8*$^{-/-}$ (*Eps8*$^{-/-}$) BMDCs is shown.
(C) Eps8 capping, but not bundling activity, is required to restore *Eps8*$^{-/-}$ BMDC protrusions in 3D. *Eps8*$^{-/-}$ (*Eps8*$^{-/-}$) BMDCs were transfected with either full-length (FL) GFP-Eps8 or the indicated mutants and treated with LPS and embedded in 1.6 mg/ml collagen type I matrix. CCL19 (1.2 μg/ml) was added in the upper part of the polymerized gel. BMDC protrusive activity was recorded as described above (see also Movie S5). Still images from representative movies are shown. At least 30 cells/experiment/condition of three independent BMDC preparations were analyzed by time lapse. The scale bar represents 10 μm.

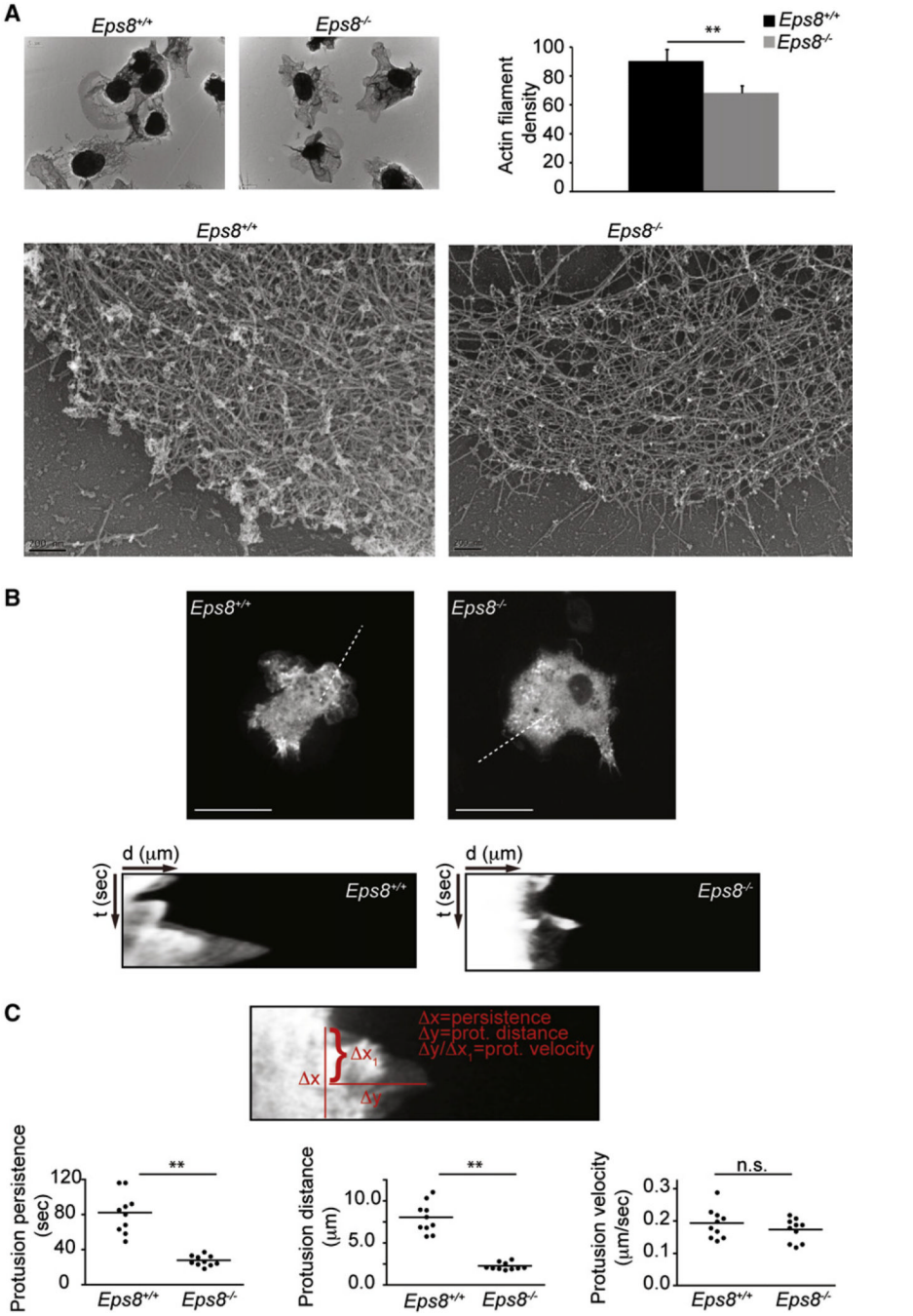

Figure 7. Eps8-Deficient BMDCs Display Reduced Density of the Lamellipodial Actin Meshwork and Reduced Protrusion Persistence

(A) *Eps8* deficiency causes a reduction in the actin filament meshwork density of BMDC protrusions. Platinum replica EM of lamellipodia of WT (*Eps8*$^{+/+}$) and *Eps8*$^{-/-}$ (*Eps8*$^{-/-}$) BMDCs plated as in Figure 6 was carried out as described in Svitkina and Borisy (1998). Low- (upper images) and high-magnification (lower images) representative images are shown. The scale bar of the lower images represents 200 nm. Actin filament density was determined as described in the Experimental Procedures. Data are expressed as mean ± SD (N = 75 areas from at least 15 cells/genotype); **p < 0.01.

(B and C) GFP-actin-infected, LPS-stimulated WT (*Eps8*$^{+/+}$) and *Eps8*$^{-/-}$ (*Eps8*$^{-/-}$) BMDCs were injected between a fetal bovine serum-coated, glass coverslip and a layer of agarose as described in Figure 6. Cells were induced to migrate toward a 2 mm afar attractor hole containing 1.2 μg/ml CCL19. BMDC migration was recorded by time-lapse microscopy. Still images from representative movies (Movie S6) of WT (*Eps8*$^{+/+}$) and *Eps8*$^{-/-}$ (*Eps8*$^{-/-}$) BMDCs are shown (B, top). Examples of kymographs performed on the indicated dotted lines (four to five different areas per cells of 10 different cells/genotype) are shown (B, bottom).

(C) Quantification of protrusion dynamics was carried out using kymograph image analysis software to determine protrusion persistence (Δx), distance (Δy), and velocity (Δy/Δx) as shown in the upper image (C). The distribution around the mean values of protrusion parameters of each of the ten cells/genotype is shown (C, lower panels); **$p < 0.01$., n.s., not significant.